INFUB - 11th European Conference on Industrial Furnaces and Boilers, INFUB-11

A kinetic study on simultaneously boosting the mass and fixed-carbon yield of charcoal production via atmospheric carbonization

Maria Zabalo Alonso[a], Khanh-Quang Tran[a,*], Liang Wang[b], Øyvind Skreiberg[b]

aDepartment of Energy and Process Engineering, Norwegian University of Science and Technology, NO-7491 Trondheim, Norway
bSINTEF Energy Research, P.O. Box 4761 Sluppen, NO-7465 Trondheim, Norway

Abstract

The mass and fixed-carbon yield of charcoal produced from woody biomass via atmospheric carbonization can be simultaneously improved by harnessing the phenomenon of secondary char formation as a result of prolonged contact time between pyrolysis gas and solid (char). In this study, the carbonization of forest residues in comparison with their stem wood was studied by means of a thermogravimetric analyzer operated non-isothermally at atmospheric pressure with a heating rate of 10K/min and a final temperature of 800ºC. Forest residue (tops and branches) and stem wood samples of Norway spruce, birch and oak trees collected from forests in Southern Norway were used as feedstock. The work focused on analyzing the effect of the process parameters (feedstock particle size, initial sample mass, and the residence time of volatiles released during the process) on the devolatilization kinetics of the carbonization process. The kinetic analysis was performed assuming the distributed activation energy model (DAEM) and three pseudo-components (hemicellulose, cellulose, and lignin).

1. Introduction

Charcoal, the main product from carbonization (slow pyrolysis) of biomass, has a wide range of applications in various industries. These applications include direct combustion of charcoal as solid fuel, gasification of charcoal for synthesis gas production, and use as reductant alternative to fossil carbon in metallurgical industry [1-3]. For the application as metallurgical reductant, it is required that the fixed-carbon content of charcoal is higher than 80 wt%. This requirement can normally be achieved by increasing the severity of carbonization (higher temperatures and/or longer carbonization times). As a result, more volatile matters of the feedstock will be released into the gas phase,

* Corresponding author. Tel.:+47-73-59-36-25; Fax: +47-73-59-35-80
E-mail address: khanh-quang.tran@ntnu.no

which is translated to more material and energy losses. Combustion of this pyrolysis gas for energy recovery is possible, but requires extra investment, which is rarely feasible for small and decentralized carbonization units. High-pressure carbonization of biomass has been proposed for improving the mass and fixed-carbon yield at the same time [4, 5]. However, the high-pressure requirement also leads to extra cost and is not that feasible for small carbonization units. On the other hand, the mass and fixed-carbon yield can be improved simply by promoting the secondary char formation from the pyrolysis gas via increasing the particle size of the feedstock [4]. It is because of the catalytic cracking effect, of the char formed in the outer layers of the fuel particle, on the nascent pyrolysis gas on its way diffusing outward. Alternatively, similar effects can be achieved by simply confining the pyrolysis gas in the reactor. The work presented in this paper aims to study the effect of prolonged contact time between nascent pyrolysis gas and char during carbonization on the mass and fixed-carbon yields of charcoal produced. The contact time is prolonged by varying process parameters (feedstock particle size, initial mass) and pyrolysis gas confinement. In addition to this, the work focuses on the use of forest residues as feedstock, which is a promising and low-cost renewable resource.

2. Material and experimental methods

2.1. Material

The biomass materials used as feedstock for the present study are forest residues (tops and branches,) and stem wood of Norway spruce, birch and oak trees from forests in Southern Norway. The collected samples were chipped and dried at 105ºC for 24 hours. The pre-dried samples were then milled and sieved to obtain powder samples of two particle ranges: d<1mm and 63µm<d<100µm. Proximate analysis to derive the volatile matter content, fixed-carbon content and ash content of the tested samples were analyzed according to procedures described in ASTM E871, E872 and D1102. Element compositions of the samples were analyzed by means of a Eurovector EA 3000 CHNS-O Elemental Analyzer. The higher heating value of the samples was measured by a bomb calorimeter (IKA C5010/5012 model), following the procedure descried in ASTM E711-87(2004).

2.2. Thermogravimetric method

A thermogravimetric analyzer (TGA), SDT Q600 model from TA Instrument, was used for studying the non-isothermal decomposition of the samples during the pyrolysis process. Two different initial sample masses were used, being 1 mg and 10 mg. Experiments with 1 mg samples were run for small particles only (63 µm<d<100 µm), whereas experiments with 10mg were run for the samples with both small and large particle sizes (63 µm<d<100 µm and d<1 mm). For each TGA run, a sample of either 1 mg or 10 mg was loaded in an alumina crucible that was then placed into the TGA furnace. Nitrogen (purity 99.999%) was used as purging gas through the TGA reactor, with a volumetric flow rate of 100mL/min, for 30 minutes before starting the heating up of the furnace. After this purging at room temperature, the furnace was heated to 105ºC and kept at this temperature for 30 minutes, followed by heating up to 800ºC with a heating rate of 10 K/min. For experiments with 10 mg of sample as initial mass, the crucible was operated in two modes: 1) open crucible (no lid), and 2) closed crucible (with lid), for studying the effect of the volatiles released from the sample during devolatilization on the char and fixed-carbon yields. The lid has small pinholes on it to allow the gas to escape and avoid possible pressure increase. Each experiment was repeated 3 three times to check the repeatability.

2.3. Kinetic evaluation method

Pyrolysis of lignocellulosic materials is a general term to indicate the decomposition process of an abundance of different and complex physical and chemical reactions that occur when the materials are thermally treated at elevated temperatures in an inert environment. However, for kinetic evaluation, it is a common practice to simplify the process, which can be described by the global scheme of Eq. (1) [6]:

$$\text{Solid biomass} \longrightarrow \text{Char} + \text{volatiles} \qquad (1)$$

The fundamental kinetic equation for the above scheme is represented by Eq. (2)

$$\frac{d\alpha}{dt} = A. e^{\frac{-E}{RT}}. f(\alpha) \tag{2}$$

where $f(\alpha)$ is the conversion function for the conversion degree, α, which is determined as the mass fraction of the decomposed solid (mass loss) or released volatiles of samples. The conversion degree α is defined by Eq. (3)

$$\alpha = \frac{m_o - m_t}{m_o - m_f} \tag{3}$$

where m_0, m_f, and m_t are the initial mass, final mass, and the mass of the sample at time t, respectively. The conversion function $f(\alpha)$ is dependent on the reaction mechanism and its different forms can be found in the literatures [6-8].

In general, lignocellulosic biomass materials are mainly composed of three components including hemicellulose, cellulose and lignin. The overall reaction rate is then described by Eq. (4) wherein c_i is the contribution factor of component i, i.e. c_1 for hemicellulose, c_2 for cellulose and c_3 for lignin.

$$\frac{d\alpha}{dt} = \sum_1^3 c_i \frac{d\alpha_i}{dt} \qquad i = 1,2,3 \tag{4}$$

For each of the components, the Distributed activation energy model (DAEM) with reaction order $n = 1$ is assumed. This model simplifies that all component reactions share the same pre-exponential coefficient and that the number of reactions is large enough, so that the activation energy can be represented by a continuous distribution function $f(E)$ [9]. Several forms of $f(E)$ can be applied to the DAEM model including Gaussian, Gamma, Weibull and Logistic distribution. Among these functions, the Gaussian function (Eq. 5) is most widely used.

$$f(E) = \frac{1}{\sigma\sqrt{2\pi}} \exp\left[-\frac{(E-E_0)^2}{2\sigma^2}\right] \tag{5}$$

where E_0 and σ are the mean activation energy and its standard deviation, respectively. The DAEM model with the reaction order of unity, $n = 1$ is described in (Eq. 6),

$$\alpha = 1 - \int_0^\infty \exp\left(-\int_{T_0}^T \frac{A}{\beta} \exp\left(-\frac{E}{RT}\right) dT\right) f(E) \, dE \tag{6}$$

where β is the heating rate. The non-linear least square method was applied to the kinetic modelling and simulation of the assumed models. The objective function to minimize is described in Eq. (7).

$$S = \sum_{i=1}^N [\left(\frac{d\alpha_i}{dt}\right)_{exp} - \left(\frac{d\alpha_i}{dt}\right)_{model}]^2 \tag{7}$$

where $\left(\frac{d\alpha_i}{dt}\right)_{exp}$ and $\left(\frac{d\alpha_i}{dt}\right)_{model}$ stand for the experimental and modelled conversion rate, N is the number of experimental points. The fit quality is appraised by Eq. (8)

$$Fit \, (\%) = \left(1 - \frac{\sqrt{\frac{S}{N}}}{[\left(\frac{d\alpha_i}{dt}\right)_{exp}] \, max}\right). 100\% \tag{8}$$

3. Results and discussion

3.1. Fuel characteristics

Table 1 presents results from the proximate and ultimate analysis of the GROT and woody biomass samples, together with their HHV values. Overall, the forest residue has higher HHV than the stem wood. This is mainly due to the higher C and lower O content of the forest residue compared to the stem wood. In addition, the forest residue have lower volatile matter (VM) but higher fixed-carbon (FC) content than the stem wood, of which the later would be better for forest residue as start material to produce charcoal for use as metallurgical reductant, considering production of charcoal with higher carbon content. Both ash content and concentration of inorganic elements of the forest residue are also higher than those of counterpart stem wood. Presence of inorganic elements will affect carbonization reactions. For example, the inorganic elements will act as catalyst to promote secondary reactions of tarry vapors [9].

Table 1. Fuel characterization of the feedstocks (dry basis)

Feedstock	Proximate analysis, wt%			Ultimate analysis, wt%					HHV (MJ/kg)	Inorganic composition (mg/kg, d.b.)					
	VM	FC	Ash	C	H	N	S	O		Si	Ca	K	Mg	P	Mn
SF	72.1	25.4	2.5	51.7	6.1	0.7	0.0	41.5	20.63	571	6004	2516	649	349	877
SW	78.0	21.4	0.6	49.6	6.4	0.1	0.0	43.8	19.64	63	1958	672	212	61	333
BF	73.8	23.5	2.7	50.7	6.3	0.8	0.0	42.1	20.84	409	5022	2002	770	543	342
BW	81.4	17.8	0.8	49.9	6.7	0.4	0.0	43.1	19.57	125	2109	725	314	165	162
OF	74.0	23.7	2.3	50.2	5.9	0.8	0.0	43.1	19.14	499	5321	1897	598	278	456
OW	80.6	18.5	1.0	49.3	6.2	0.1	0.0	44.5	18.20	98	2014	678	389	149	409

VM: Volatile matter; FC: Fixed-carbon

3.2. Kinetic analysis

The kinetic analysis carried out yielded the results shown in the Tables 2-6 below, where S.D. is the average value of the square differences.

Table 2. Sample mass 1mg, particle size 63µm<d<100µm, open crucible.

	c_i	E_{0i} (kJ/mol)	A_i (min^{-1})	σ (kJ/mol)	S.D.	Fit (%)
SW	0.28	98.65	4.63E+09	11.05		
	0.38	251.00	3.37E+21	29.12	2.07E-03	98.36
	0.10	52.00	5.85E+04	5.12		
BW	0.30	92.33	2.37E+09	10.27		
	0.38	241.97	7.98E+20	28.24	2.49E-03	98.09
	0.10	56.11	1.22E+05	3.15		
OW	0.23	95.67	1.23E+10	10.26		
	0.27	117.79	9.98E+10	13.16	1.80E-03	97.49
	0.18	58.36	1.25E+05	5.02		
SF	0.29	74.97	7.65E+07	7.76		
	0.31	162.39	4.01E+14	17.62	6.00E-04	98.34
	0.12	35.63	6.37E+03	3.78		
BF	0.24	79.72	3.33E+08	8.17		
	0.31	141.79	8.69E+12	15.73	7.01E-04	98.25
	0.12	39.77	1.11E+04	4.08		
OF	0.29	99.14	1.63E+10	10.65		
	0.31	156.32	1.34E+14	17.81	9.59E-04	98.29
	0.15	42.32	1.18E+04	3.64		

Table 3. Sample mass 10mg, particle size 63μm<d<100μm, open crucible.

	c_i	E_{0i} (kJ/mol)	A_i (min^{-1})	σ (kJ/mol)	S.D.	Fit (%)
SW	0.25	106.82	2.53E+10	11.87		
	0.38	256.82	1.66E+22	29.96	2.66E-03	98.07
	0.13	40.30	1.65E+04	4.00		
BW	0.31	94.42	3.74E+09	10.33		
	0.38	249.61	3.73E+21	28.79	1.43E-03	98.46
	0.11	58.42	3.07E+05	2.50		
OW	0.27	89.50	2.78E+09	9.47		
	0.36	151.87	6.82E+13	16.54	8.74E-04	99.79
	0.18	37.98	8.38E+03	3.00		
SF	0.27	80.25	2.60E+08	3.10		
	0.28	176.04	5.79E+15	19.27	7.92E-04	98.02
	0.18	40.35	1.58E+04	1.77		
BF	0.27	84.80	1.02E+09	2.56		
	0.30	140.90	7.98E+12	15.42	5.34E-04	98.31
	0.18	40.69	1.67E+04	2.18		
OF	0.27	104.60	6.13E+10	2.86		
	0.30	157.74	2.04E+14	18.00	6.12E-04	98.67
	0.18	37.59	7.43E+03	3.23		

Table 4. Sample mass 10mg, particle size d<1mm, open crucible.

	c_i	E_{0i} (kJ/mol)	A_i (min^{-1})	σ (kJ/mol)	S.D.	Fit (%)
SW	0.28	115.40	1.90E+11	12.5		
	0.33	219.72	1.01E+19	25.95	3.68E-03	97.67
	0.15	42.42	1.50E+04	4.00		
BW	0.33	102.37	2.07E+10	11.13		
	0.38	243.41	1.18E+21	28.13	1.39E-03	98.40
	0.10	58.00	2.78E+05	2.32		
OW	0.25	116.03	5.05E+11	12.77		
	0.34	209.34	3.40E+18	24.28	1.79E-03	99.81
	0.18	52.56	7.82E+04	4.20		
SF	0.27	84.78	9.62E+08	3.98		
	0.31	128.82	6.93E+11	14.08	5.91E-04	98.30
	0.17	38.92	1.11E+04	3.91		
BF	0.24	93.26	5.38E+09	10.01		
	0.31	152.90	6.58E+13	16.88	9.86E-04	98.03
	0.17	54.08	1.63E+05	5.81		
OF	0.24	101.18	2.10E+10	10.88		
	0.32	160.17	2.59E+14	18.13	6.51E-04	98.62
	0.17	49.02	5.42E+04	2.96		

Table 5. Sample mass 10mg, particle size 63μm<d<100μm, closed crucible.

	c_i	E_{0i} (kJ/mol)	A_i (min^{-1})	σ (kJ/mol)	S.D.	Fit (%)
SW	0.21	107.17	3.15E+10	11.89		
	0.34	258.95	2.01E+22	30.15	1.15E-03	98.65
	0.12	55.40	1.50E+05	5.59		
BW	0.22	100.09	9.87E+09	11.11		
	0.33	253.00	7.96E+21	29.39	1.14E-03	98.55
	0.13	62.15	5.61E+05	2.56		
OW	0.25	100.58	3.20E+10	10.77		
	0.29	143.70	1.44E+13	15.90	1.96E-03	96.53
	0.16	57.57	1.90E+05	2.97		
SF	0.21	98.39	1.58E+10	2.90		
	0.28	151.84	6.12E+13	16.71	1.96E-03	96.69
	0.18	58.38	2.66E+05	2.41		
BF	0.23	89.09	2.30E+09	2.50		
	0.28	149.49	3.95E+13	3.03	1.89E-03	96.50
	0.16	60.60	4.06E+05	2.7		

Table 6. Sample mass 10mg, particle size d<1mm, closed crucible.

	c_i	E_{0i} (kJ/mol)	A_i (min^{-1})	σ (kJ/mol)	S.D.	Fit (%)
SW	0.28	103.49	1.38E+10	11.20		
	0.34	265.79	6.17E+22	30.90	1.25E-03	98.59
	0.13	52.95	9.01E+04	5.61		
BW	0.23	110.62	1.16E+11	12.40		
	0.34	262.82	5.05E+12	30.79	1.46E-03	98.52
	0.13	58.82	3.05E+05	5.92		
OW	0.23	119.06	9.96E+11	13.05		
	0.36	202.76	1.00E+18	23.39	9.21E-04	98.67
	0.16	55.73	1.41E+05	3.60		
SF	0.23	95.27	5.44E+09	2.45		
	0.29	188.80	5.05E+16	21.12	1.69E-03	97.39
	0.17	57.29	2.04E+05	5.82		
BF	0.21	96.05	7.34E+09	2.42		
	0.27	178.52	8.35E+15	20.07	1.69E-03	97.39
	0.17	56.99	2.02E+05	5.80		
OF	0.21	104.55	5.70E+10	2.09		
	0.32	174.84	4.98E+15	19.82	1.47E-03	97.99
	0.18	59.80	2.92E+05	3.50		

3.3. Discussion

Overall, the obtained kinetic data are comparable with values from literature with observations and discussion as below [10-12]. Repeatability of the stem wood experiments was good, while it was lower for the forest residue experiments. Also the fit values were in general lower for the forest residue experiments.

Regarding possible influence of increased contact time between the pyrolysis gas and the char matrix, increasing the char and fixed-carbon yield, the following increasing trend from lowest to highest yields could be expected: 1) small particles, low sample mass, open crucible, 2) small particles large sample mass, open crucible, 3) large particles, large sample mass, open crucible, 4) small particles, large sample mass, closed crucible, and 5) large particles, large sample mass, closed crucible. In addition, as secondary char forming reactions are expected from the cellulose and lignin fractions of the biomass, it could be expected that the contribution factors calculated for these would decrease somewhat with increasing char yields [13]. Other main influencing factors are the amount of hemicellulose, cellulose and lignin in the different wood species and their forest residue fraction, as well as the ash content and especially the catalytic fraction of the ash.
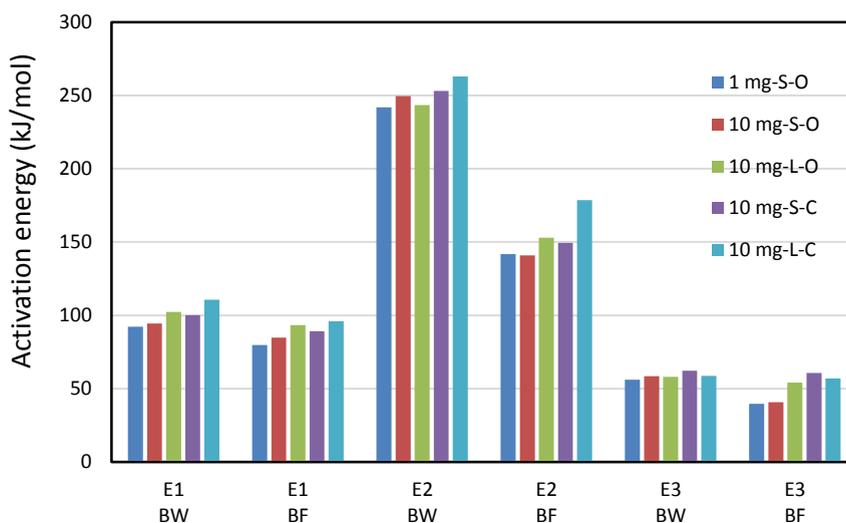

Fig. 1. Activation energies for birch wood (BW) and birch forest residue (BF) for the five severity conditions (sample size, mg; particle size, small (s) or large (l); open crucible (o) or closed crucible (c)). E1: hemicellulose, E2: cellulose, E3: lignin.

Regarding activation energies, significantly lower activation energies were obtained for forest residue samples than for their counterpart stem wood samples, caused by much higher amount of catalytic ash elements in the forest residue ashes. Also, a clear tendency towards increasing activation energies for hemicellulose, cellulose and lignin with increasing favorable char and fixed-carbon yield conditions as outlined in point 1) to 5) above was observed. These observations are shown for birch wood (BW) and birch forest residue (BF) in Fig. 1.

When grouping the activation energies for 1mg, 10mg, small particles, large particles, open crucible and closed crucible and calculating mean activation energies within the different groups, the result becomes as shown in Fig. 2, for birch. In the figure, clear trends can be seen, i.e. the activation energy increases with increasing sample mass and particle size and when a lid is used on the crucible.
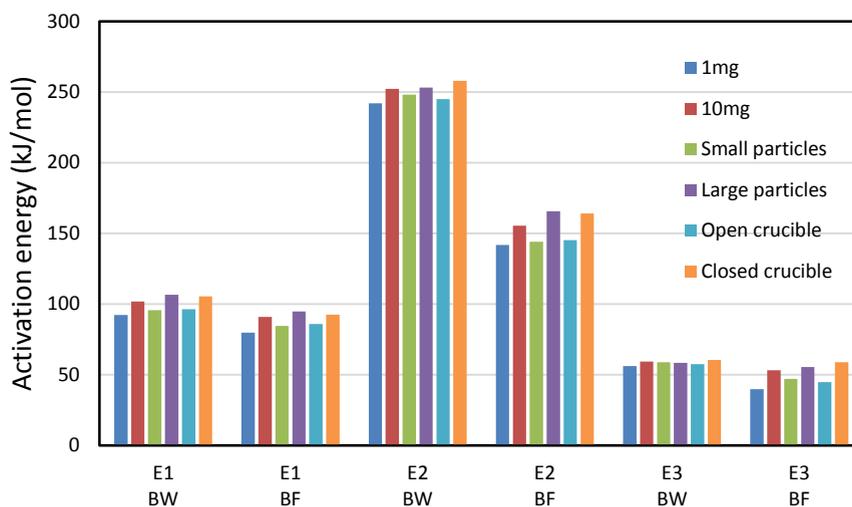

Fig. 2. Activation energies for birch wood (BW) and birch forest residue (BF) when grouping the activation energies for 1mg, 10mg, small particles, large particles, open crucible and closed crucible and calculating mean activation energies within the different groups.

Regarding char yields, i.e. 1 minus the contribution factors for hemicellulose, cellulose and lignin, increased char yields were found for the forest residue samples compared to their counterpart stem wood. Also, a trend of increasing char yields with increasing severity condition, i.e. confinement of tarry vapors and enhancement of secondary reactions, was found. This is consistent with also increase in fixed-carbon yields as reported in our recent work [14,15].

Regarding contribution factors, the contribution factor for cellulose is lower for forest residue than that of stem wood. Also for cellulose, a trend of decreasing contribution condition with increasing severity factor was found. No clear trend was found for hemicellulose, and somewhat more unexpected, for lignin. The various trends for spruce are similar to the trends for birch. In the case of oak, the trends were not so clear, and further work is needed to assess why.

4. Conclusions

Higher overall reactivity of spruce and birch forest residue samples was observed in comparison with their counterparts stem wood samples. It is indicated by the lower values of the activation energy registered for the forest residue samples. This is partially related to higher amount of ash forming elements in the forest residues, which act as catalyst and promote decomposition reaction and lowers the needed minimum energy amount for the reaction to get started.

Regarding the obtained values of kinetic parameters, relatively small differences were observed for stem wood and forest residues, which are from hardwood (birch and oak) and softwood (spruce) trees respectively.

For one studied sample, considerable different kinetic parameters were calculated from experiments using different sample initial weight and particles size. This effect was considered to become significant when increasing sample mass and particle size of the samples, resulting in a shift from kinetically controlled reactions to reactions

dominated by heat and mass transfer. Therefore, the proposed kinetic evaluation and modelling are not enough to simulate the decomposition behaviors of samples with large sample mass and particle size. It partially explains variations of the kinetic parameters obtained from one sample but with different experimental conditions.

Regarding the effect of the lid, a clear tendency was observed regarding the influence of the prolonged contact time of tarry vapors with the char matrix, resulting in increased char yields and influence on contribution factors as well as derived activation energies.

The results from this study show that the yield of charcoal and fixed-carbon can be enhanced by tuning carbonization process conditions, to enhance secondary char forming reactions. A boost in charcoal and fixed-carbon yields can be achieved by increasing the particle/sample size and forcing confinement of tarry vapors and increased contact time between these and the char matrix. For a specific carbonization reactor the influencing factors on the charcoal and fixed-carbon yields need to be optimized. Complicated models, accounting for the impacts of sample size, particle size and prolonged vapor residence time on the interactions of volatiles with the solid substrate, are needed to evaluate biomass pyrolysis/carbonization reactions and products yields.

Acknowledgements

References

[1] Altun NE, Kök MV, Hicyilmaz C. Effect of Particle Size and Heating Rate on the Combustion of Silopi Asphaltite. *Energy & Fuels*. 2002; **16** :785-90.
[2] Wang L, Várhegyi G, Skreiberg Ø, Li T, Grønli M, Antal MJ. Combustion Characteristics of Biomass Charcoals Produced at Different Carbonization Conditions: A Kinetic Study. *Energy & Fuels*. 2016; **30**:3186-97.
[3] Monsen B, Grønli M, Nygaard L, Tveit H. The use of biocarbon in the Norwegian ferroalloy production. The Ninth International Ferroalloys Congress and the Manganese Health Issues Symposium. 2001.
[4] Wang L, Skreiberg Ø, Gronli M, Specht GP, Antal MJ. Is Elevated Pressure Required to Achieve a High Fixed-Carbon Yield of Charcoal from Biomass? Part 2: The Importance of Particle Size. *Energy & Fuels*. 2013; **27**:2146-56.
[5] Van Wesenbeeck S, Higashi C, Legarra M, Wang L, Antal MJ. Biomass Pyrolysis in Sealed Vessels. Fixed-Carbon Yields from Avicel Cellulose That Realize the Theoretical Limit. *Energy & Fuels*. 2016; **30**:480-91.
[6] Di Blasi C. Modeling chemical and physical processes of wood and biomass pyrolysis. *Progress in Energy and Combustion Science*. 2008; **34**:47-90.
[7] Grønli M, Várhegyi G, Di Blasi C. Thermogravimetric Analysis and Devolatilization Kinetics of Wood. Industrial & Engineering Chemistry Research. 2002; 41(17):4201-8.
[8] Branca C, Albano A, Di Blasi C. Critical evaluation of global mechanisms of wood devolatilization. Thermochimica Acta. 2005; **429**:133-41.
[9] Várhegyi G, Antal MJ, Jakab E, Szabó P. Kinetic modeling of biomass pyrolysis. Journal of Analytical and Applied Pyrolysis. 1997; **42**:73-87.
[10] Bennadji H, Smith K, Serapiglia MJ, Fisher EM. Effect of Particle Size on Low-Temperature Pyrolysis of Woody Biomass. *Energy & Fuels*. 2014; **28**:7527-37.
[11] Tran K-Q, Bach Q-V, Trinh TT, Seisenbaeva G. Non-isothermal pyrolysis of torrefied stump – A comparative kinetic evaluation. Applied Energy. 2014; **136**:759-66.
[12] Tapasvi D, Khalil R, Várhegyi G, Tran K-Q, Grønli M, Skreiberg Ø. Thermal Decomposition Kinetics of Woods with an Emphasis on Torrefaction. *Energy & Fuels*. 2013; **27**:6134-45.
[13] Pattanotai T, Watanabe H, Okazaki K. Experimental investigation of intraparticle secondary reactions of tar during wood pyrolysis. Fuel. 2013; **104**:468-75.
[14] Wang L, Skreiberg Ø, Van Wesenbeeck S, Grønli M, Antal MJ. Experimental Study on Charcoal Production from Woody Biomass. Energy & Fuels. 2016; **30**:7994-8008.
[15] Tran K-Q, Alonso MZ, Wang L, Skreiberg Ø. Simultaneously boosting the mass and fixed-carbon yields of charcoal from forest residue via atmospheric carbonization. Energy Procedia, in press.